CHEMISTRY OF MATERIALS

COMMUNICATION

pubs.acs.org/cm

Template-Free Formation of Monodisperse Doughnut-Shaped Silica Microparticles by Droplet-Based Microfluidics

Aiping Fang,*[,†] Cédric Gaillard,[‡,§] and Jean-Paul Douliez[‡]

[†]NANO, [‡]ISD, and [§]BIBS Microscopies, UR 1268, Biopolymères Interactions Assemblages, INRA, rue de la Géraudière, 44316 Nantes, France

KEYWORDS: droplet microfluidics, solvent diffusion, sol−gel transition, doughnut-shaped silica

Silica materials have been extensively investigated because of their applications in a wide variety of areas, such as large-molecule catalysis, biomolecule separations, and development of sensors and devices. Since the early 1990s,[1] mesoporous silica has drawn much attention because of its extraordinary functionalities (mesoporosity,[2] chirality,[3] surface functionalities,[4] etc.). To control their pore size and morphology,[5] soft matters, such as amphiphilic surfactants, block polymers, and biomacromolecules, have been successfully used as templates for the synthesis of hollow silica spheres.[6] The unique properties of these mesoporous silica particles, such as their high surface area, large pore volume, tunable pore size with a narrow distribution, and good chemical and thermal stability, render them suitable candidates for various controlled release applications. However, their polydispersity, either in size or shape, presents a major challenge in understanding and controlling the mass-transport properties. Additionally, nonspherical silica particles, such as disklike ones, will inspire new research in the fields of nanomedicine.[7]

The emerging microfluidic technique provides a straightforward and robust approach to the formation of highly monodisperse emulsion droplets, one at a time, with an incomparable degree of control over size. Additionally, in the droplet formation, the ability to control the local flow field via the fabrication of complex microscale geometries enables control over the deformation and breakup of every individual droplet, thus allowing control over the shape, morphology, internal structures,[8] and chemistry (isotropic and anisotropic/Janus particles).[9] Microfluidic emulsion droplets have been demonstrated as both morphological templates[10] and chemical reactors[11] for the synthesis of monodisperse silica microspheres. It remains a challenge in controlling the shape of particles at the microscale, as the effect of surface tension favors spherical particles. Although droplet-based microfluidics has been successfully applied for the controlled fabrication of monodisperse nonspherical polymer particles,[12] it has not been exploited for nonspherical silica particles. Here, we describe a simple droplet-based microfluidic approach for the controlled formation of doughnut-shaped silica microparticles. Uniform silica sol emulsion droplets in an organic phase, dimethyl carbonate (DMC), were generated. As a result of its water immiscibility and solubility (solubility of water in DMC, 2.9 wt %),[13] the emulsion droplets subsequently underwent in situ rapid water diffusion within the microfluidic channel, therefore inducing buckling instability and resulting in a doughnut-shape. This is a facile and general approach with good control in shape and size. The silica microparticles prepared in this way are monodisperse in both size and shape.

A flow focusing polydimethylsiloxane (PDMS) device is used to generate W/O emulsion droplets (see Figure 1; its fabrication details can be found in previous work[14]). The serpentine channel has a cross-sectional dimension of 200 μm (width) × 80 μm (height). Silica sol was achieved by mixing 2.0 mL tetraethyl orthosilicate (TEOS, 99.0%, Fluka) and 0.2 mL triethyl amine (99.5%, Fluka) with 10.0 mL water (Milli Q, 18 MΩ cm) under stirring at room temperature until one single homogeneous phase appeared (∼5 h). The oil phase DMC was supplied to the PDMS device through inlet 1 using a digitally controlled syringe pump (Harvard Apparatus PHD 2000, U.S.A.), with a flow rate varying from 3.00 to 5.00 mL/h. The precursor solution was supplied to the PDMS device through inlet 2 in the same manner, with a flow rate varying from 0.02 to 0.10 mL/h, where it is emulsified into droplets by the continuous oil phase. Unless otherwise stated, the silica sol was directly supplied to the device without further dilution at a flow rate of 0.05 mL/h, while that of the continuous phase was supplied at 3.00 mL/h. An Olympus IX51 inverted microscope equipped with a digital camera (Sony, SCD-SX90) was used for high-speed imaging. The evolution of a droplet is also displayed in Figure 1.

Initially, spherical emulsion droplets are generated (Figure 1a), and as a result of water diffusion into the continuous DMC phase, the droplets gradually shrink to smaller sizes when they travel downstream inside the serpentine microfluidic channel (Figure 1b) . After traveling in the serpentine channel for 3.8 s, as indicated in Figure 1c, the droplets start deforming, depicting a condensation process. Buckling along the cross-flow direction is subsequently observed, while the droplets progressively develop into a discoidal shape (Figure 1d). With concomitant solvent diffusion into oil phase, the droplets shrink further until solidification (Figure 1e−f). Once solidified, the particle size and morphology remain unchanged. The particles were collected from outlet 3 for further characterization.

Remarkably, the spherical emulsion droplets eventually solidify to form doughnut-shaped particles, as observed in Figure 2 by optical microscopy and scanning electron microscopy (SEM) images. The as-formed particles are monodisperse in both size and shape. The size distribution of the particles in Figure 2c

Received: July 26, 2011
Revised: September 21, 2011
Published: October 07, 2011

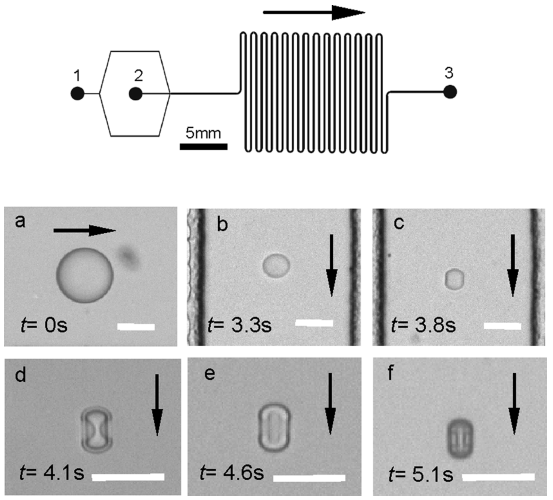

Figure 1. Schematic of the PDMS device used for this work (top). Evolution of a droplet (bottom) as it travels downstream: (a) droplet generation; (b) shrinkage; (c) deformation; (d) buckling; (e) condensation; and (f) solidification. The time indicates the actual time from the droplet generation. The arrows depict flow direction in channels. The dark edges in parts b and c correspond to the side wall of the serpentine channel. Scale bar: 50 μm.

exhibits one well-defined peak centered around 25 μm with a coefficient of variation of 3.5% (Figure 2d, the outer diameter of silica particles is measured by doubling the distance from the edge of the doughnut to its center). These particles are obtained from droplets with the initial size of 75 μm; after solidification, their final size is approximately one-third of that of original droplets. The side and tilted view of the particles from the optical photograph in Figure 2a (indicated by open and filled arrows, respectively) help to understand the microstructures of the particle: two cavities symmetrically rest on the two facades of the disk and are separated by a thin central membrane; these are also clearly disclosed in the confocal fluorescence image in Figure 2f. The structure is obviously different from that of torus.[12a]

The size of the particles depends on the initial size and concentration of silica sol droplets, while the size of the original droplets depends on, for instance, the dimensions and geometry of the microchannel and the flow rates of the disperse and oil phases. Using the microfluidic device, as shown in Figure 1, we are able to achieve silica particles with a size ranging 15−50 μm, simply by varying the flow rate of the continuous phase from 5.00 mL/h to 3.00 mL/h and that of disperse phase from 0.02 mL/h to 0.10 mL/h. Because solidification is induced by water diffusion, it is expected that a diluted sol will lead to more important shrinkage and thus smaller particles. Indeed, particles with a size of 7 μm (Figure 2b) were successfully formed by using a sol diluted 200 times, corresponding to 10 times shrinkage from the original droplet size. Nevertheless, further dilution of the sol did not bring a further decreased size. In particular, a trial with 10 000 times diluted sol unexpectedly offered similar 10 times shrinkage, but it also produced a wrinkled structure indicative of a low relative density (image not shown).[15] These results show that alternative experimental parameters have to be manipulated (e.g., channel dimension, viscosity of the fluids, and use of surfactant) to fabricate particles with a size less than 5 μm.

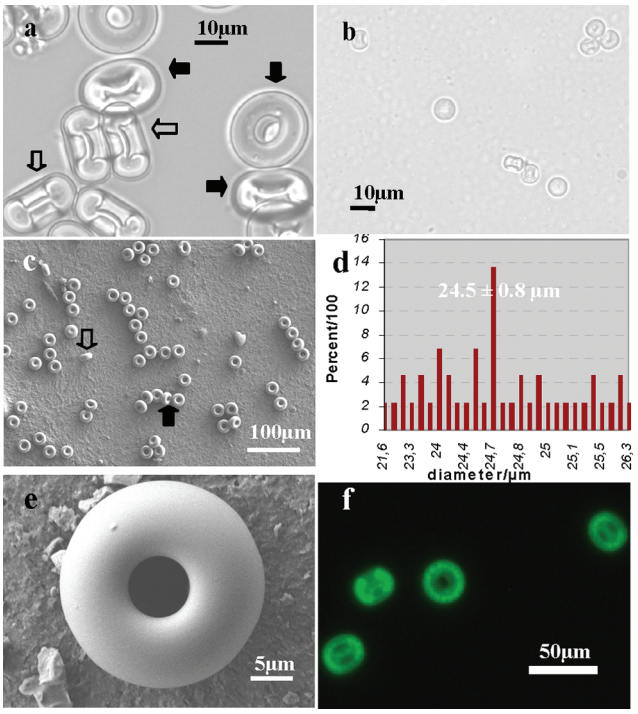

Figure 2. Monodisperse doughnut-shaped silica particles as shown by optical microscope with a size of 25 μm (a) and 7 μm (b). (c and e) SEM images. (d) Size distribution of particles in part c. (f) Confocal fluorescence microscopy image denoting the thin central membrane microstructure. The particles were formed with a disperse phase flow rate of 0.05 mL/h and a continuous phase flow rate of 3.00 mL/h. Silica particles 7 μm in size were achieved similarly, except using a sol diluted at 200 times; fluorescent silica was achieved by a sol mixed with FITC dye. Open and filled arrows indicate the side and titled view of the doughnut-shaped silica, respectively. The images were taken without a calcination step.

It is interesting to investigate the formation mechanism of the doughnut-shaped silica. The evolution of a droplet in Figure 1 provides us with a clue regarding the drying dynamics of droplets. As seen from Figure 1a and b, the droplet shrinks nearly isotropically at the first water loss stage. Then, a deformation is observed, where the spherical object transforms into a discoidal one (Figure 1c). Obviously, there exists inhomogeneity and the droplet tends to flatten in the cross-flow direction. The drying of complex fluids such as colloidal sol dispersions involves complex spatial and temporal evolutions that are related to a large number of microscopic phenomena, coupling evaporation process, hydrodynamics, and mechanical instabilities.[16] The successive mechanisms during the desiccation of sessile drops have been experimentally revealed before[17] and could be equally applied here: as the droplet progressively shrinks as a result of solvent loss, the solute concentration near the water/oil interface becomes high; further accumulation of the solute leads to the local formation of a porous gelled skin. This glassy outer layer behaves as an elastic shell, which, however, does not impede diffusion. As the volume it encloses decreases, compressing the surface as it flattens costs more and more energy, and it becomes energetically more favorable to convert a part of the stretching energy into bending energy. As a result, a buckling instability takes place, and the shell bends (Figure 1c). Later, the droplet surface area remains almost constant while its volume keeps

dx.doi.org/10.1021/cm202145s |*Chem. Mater.* 2011, 23, 4660–4662

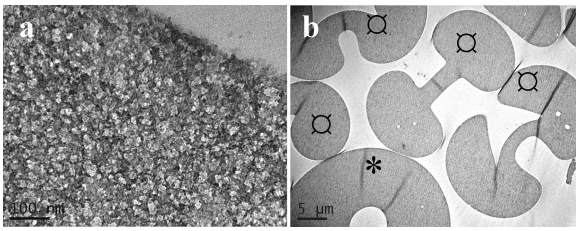

Figure 3. TEM images at different magnifications of the silica particles showing its amorphous nature consisting of nanoclusters at ~25 nm (a) and its microstructures (b) at top view (*) or side view (¤). Silica particles were cured in epoxy resin, followed by sectioning into ultrathin slices of ~50 nm in thickness.

decreasing (Figure 1d−e). The depression at both sides of the droplet deepens, and droplet undergoes invagination symmetrically. Eventually, solvent is removed, and the droplet is solidified with further decreases in its size, as seen in Figure 1f, leading to the formation of the doughnut-shaped microstructure.

The fact that the nearly symmetric invaginations do not yield a hole is proved by TEM observations. Silica particles were cured in epoxy resin and sectioned into ultrathin slices for TEM observations. Figure 3 elucidates the unique morphology of the monodisperse silica particles. The amorphous nature of the silica particles is clear from Figure 3a, consisting of nanoclusters at a size of ~25 nm. In Figure 3b, not all of the two cavities are symmetric, which is equally observed from the optical microscope image in Figure 2a. For each doughnut-shaped silica, a thin, unbroken membrane separates the two cavities. The thickness of the membrane is 2−3 μm. This unique microstructure is different from that of a toroidal structure punctured with a hole.[12a]

In summary, we introduce a general one-step approach for the controlled formation of monodisperse doughnut-shaped silica particles with a size ranging 7−50 μm. The solvent loss of a silica sol triggers gel transition. A buckling instability at the interface induces progressive invagination at the cross-flow direction, yielding the doughnut-shaped structure. To the best of our knowledge, this monodisperse doughnut-shaped silica microparticle has not been reported previously. Moreover, the kinetics of solvent removal could be well controlled by using DMC with different water contents (e.g., anhydrous or water-saturated DMC), which would be utile to trace the interface-templated self-assembly process in silica. According to the drying hydrodynamics, it would also be plausible to generate silica particles with other shapes (e.g., sphere, dimpled sphere, pancake, torus)[18] simply by tuning the sol concentration, sol particle size, electrolytes, and viscosity of the disperse phase, etc. We think that this microfluidic approach can offer new opportunities to achieve shape-specific silica particles with well-defined size, generating a wide interest in controlled release, sensing, materials, and drying kinetics.

AUTHOR INFORMATION

Corresponding Author

*Tel: +33240675144. Fax: +33240675043. E-mail: aiping.fang@nantes.inra.fr.

ACKNOWLEDGMENT

The authors thank Dr. C. Gosse at LPN-CNRS for comments, advice, and useful discussion. Mr. F. Monti and Dr. P. Tabeling are acknowledged for access to the facilities in ESPCI for microfabrication of replica models. Mr. P. Papineau is also acknowledged for kind assistance in image acquisition software.

REFERENCES

(1) (a) Kresga, C. T.; Leonowicz, M. E.; Roth, W. J.; Vartuli, J. C.; Beck, J. S. *Nature* **1992**, *359*, 710. (b) Beck, J. S.; Vartuli, J. C.; Roth, W. J.; Leonowicz, M. E.; Kresga, C. T.; Schmitt, K. D.; Chu, C. T. W.; Olson, D. H.; Sheppard, E. W.; McCullen, S. B.; Higgins, J. B.; Schlenker, J. L. *J. Am. Chem. Soc.* **1992**, *114*, 10834. (c) Yanagisawa, T.; Shimizu, T.; Kuroda, K.; Kato, C. *Bull. Chem. Soc. Jpn.* **1990**, *63*, 988.

(2) Wan, Y.; Zhao, D. *Chem. Rev.* **2007**, *107*, 2821and references therein.

(3) (a) Jung, J. H.; Ono, Y.; Hanabusa, K.; Shinkai, S. *J. Am. Chem. Soc.* **2000**, *122*, 5008. (b) Jung, J. H.; Kobayashi, H.; Masuda, M.; Shimizu, T.; Shinkai, S. *J. Am. Chem. Soc.* **2001**, *123*, 8785. (c) Che, S.; Liu, Z.; Ohsuna, T.; Sakamoto, K.; Terasaki, O.; Tatsumi, T. *Nature* **2004**, *429*, 281. (d) Jin, H.; Liu, Z.; Ohsuna, T.; Terasaki, O.; Inoue, Y.; Sakamoto, K.; Nakanishi, T.; Ariga, K.; Che, S. *Adv. Mater.* **2006**, *18*, 593.

(4) Vivero-Escoto, J. L.; Slowing, I. I.; Trewyn, B. G.; Lin, V. S.-Y. *Small* **2010**, *6*, 1952; and references therein.

(5) (a) Tanev, P. T.; Liang, Y.; Pinnavaia, T. J. *J. Am. Chem. Soc.* **1997**, *119*, 8616. (b) Huh, S.; Wiench, J. W.; Yoo, J.-C.; Pruski, M.; Lin, V. S.-Y. *Chem. Mater.* **2003**, *15*, 4247. (c) Bellomo, E. G.; Deming, T. J. *J. Am. Chem. Soc.* **2006**, *128*, 2276. (d) Yuan, J.-J.; Mykhaylyk, O. O.; Ryan, A. J.; Armes, S. P. *J. Am. Chem. Soc.* **2007**, *129*, 1717. (e) Khanal, A.; Inoue, Y.; Yada, M.; Nakashima, K. *J. Am. Chem. Soc.* **2007**, *129*, 1534. (f) Guo, X.; Deng, Y.; Tu, B.; Zhao, D. *Langmuir* **2010**, *26*, 702.

(6) (a) Caruso, F.; Caruso, R. A.; Mőhwald, H. *Science* **1998**, *282*, 1111. (b) Shiomi, T.; Tsunoda, T.; Kawai, A.; Chiku, H.; Mizukami, F.; Sakaguchi, K. *Chem. Commun.* **2005**, 5325. (c) Wang, Y.; Angelatos, A. S.; Caruso, F. *Chem. Mater.* **2008**, *20*, 848. (d) Wang, J.; Li, F.; Zhou, H.; Sun, P.; Ding, D.; Chen, T. *Chem. Mater.* **2009**, *21*, 612. (e) Qi, G.; Wang, Y.; Estevez, L.; Switzer, A. K.; Duan, X.; Yang, X.; Giannelis, E. *Chem. Mater.* **2010**, *22*, 2693–2695.

(7) Li, T.; Hu, W.; Liu, Y.; Huang, G.; Sumer, B. D.; Gao, J. *Exp. Biol. Med.* **2011**, *236*, 20.

(8) Nie, Z.; Xu, S.; Seo, M.; Lewis, P. C.; Kumacheva, E. *J. Am. Chem. Soc.* **2005**, *127*, 8058.

(9) (a) Nisisako, T.; Torii, T.; Takahashi, T.; Takizawa, Y. *Adv. Mater.* **2006**, *18*, 1152. (b) Shepherd, R. F.; Conrad, J. C.; Rhodes, S. K.; Link, D. R.; Marquez, M.; Weitz, D. A.; Lewis, J. A. *Langmuir* **2006**, *22*, 8618. (c) Nie, Z.; Li, W.; Seo, M.; Xu, S.; Kumacheva, E. *J. Am. Chem. Soc.* **2006**, *128*, 9408.

(10) (a) Carroll, N. J.; Tathod, S. B.; Derbins, E.; Menndez, S.; Weitz, D. A.; Petsev, D. N. *Langmuir* **2008**, *24*, 658. (b) Lee, I.; Yoo, Y.; Cheng, Z.; Jeong, H.-K. *Adv. Funct. Mater.* **2008**, *18*, 4014.

(11) Chokkalingam, V.; Weidenhof, B.; Krämer, M.; Maier, W. F.; Herminghaus, S.; Seemann, R. *Lab Chip* **2010**, *10*, 1700.

(12) (a) Wang, B.; Shum, H. C.; Weitz, D. A. *ChemPhysChem* **2009**, *10*, 641. (b) Shum, H. C.; Abate, A. R.; Lee, D.; Studart, A. R.; Wang, B.; Chen, C.-H.; Thiele, J.; Shah, R. K.; Krummel, A.; Weitz, D. A. *Macromol. Rapid Commun.* **2010**, *31*, 108; and references therein.

(13) Rondeau, E.; Cooper-White, J. J. *Langmuir* **2008**, *24*, 6937.

(14) Fang, A.; Cathala, B. *Colloids Surf., B* **2011**, *82*, 81.

(15) Tsapis, N.; Bennett, D.; Jackson, B.; Weitz, D. A.; Edwards, D. A. *Proc. Natl. Acad. Sci. U.S.A.* **2002**, *99*, 12001.

(16) Brinker, C. J.; Scherer, G. W. *Sol−Gel Science*; Academic Press: New York, 1990; pp 453−488.

(17) Pauchard, L.; Couder, Y. *Europhys. Lett.* **2004**, *66*, 667.

(18) Velev, O. D.; Lenhoff, A. M.; Kaler, E. W. *Science* **2000**, *287*, 2240.